Accepted Manuscript

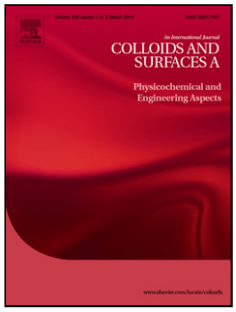

Title: Proposed molecular model for electrostatic interactions between insulin and chitosan. Nano-complexation and activity in cultured cells

Authors: Cecilia Prudkin Silva, Jimena H. Martínez, Karina D. Martínez, María E. Farías, Federico Coluccio Leskow, Oscar E. Pérez

PII: S0927-7757(17)30939-1
DOI: https://doi.org/10.1016/j.colsurfa.2017.10.040
Reference: COLSUA 21998

To appear in: *Colloids and Surfaces A: Physicochem. Eng. Aspects*

Received date: 24-8-2017
Revised date: 13-10-2017
Accepted date: 18-10-2017

Please cite this article as: Cecilia Prudkin Silva, Jimena H.Martínez, Karina D.Martínez, María E.Farías, Federico Coluccio Leskow, Oscar E.Pérez, Proposed molecular model for electrostatic interactions between insulin and chitosan.Nano-complexation and activity in cultured cells, Colloids and Surfaces A: Physicochemical and Engineering Aspects https://doi.org/10.1016/j.colsurfa.2017.10.040

Proposed molecular model for electrostatic interactions between insulin and chitosan. Nano-complexation and activity in cultured cells

Cecilia Prudkin Silva[a,b], Jimena H Martínez[a,b], Karina D Martínez[c,d], María E Farías[c,e,f], Federico Coluccio Leskow[a,b,g], Oscar E Pérez[a,b,h*]

[a] Universidad de Buenos Aires, Facultad de Ciencias Exactas y Naturales, Departamento de Química Biológica, Buenos Aires, Argentina.

[b] CONICET, Universidad de Buenos Aires, Instituto de Química Biológica de la Facultad de Ciencias Exactas y Naturales (IQUIBICEN), Buenos Aires, Argentina.

[c] Universidad de Buenos Aires, Facultad de Ciencias Exactas y Naturales, Departamento de Industrias, Buenos Aires, Argentina.

[d] CONICET. Universidad de Buenos Aires, Instituto de Tecnología de Alimentos y Procesos Químicos (ITAPROQ), Buenos Aires Argentina.

[e] Departamento de Tecnología, Universidad Nacional de Luján, Ruta 5 y 7, Luján (6700), Provincia de Buenos Aires, Argentina.

[f] CIC. Comisión de Investigaciones Científicas de la Provincia de Buenos Aires

[g] Departamento de Ciencias Básicas, Universidad Nacional de Luján, Luján, Buenos Aires, Argentina.

[h] Departamento de Desarrollo Productivo y Tecnológico, Universidad Nacional de Lanús, Buenos Aires, Argentina.

*Corresponding author: Oscar E. Pérez.
Tel: +54 11 45763342; fax: +54 11 45763342.
E-mail address: oscarperez@qb.fcen.uba.ar

Graphical abstract

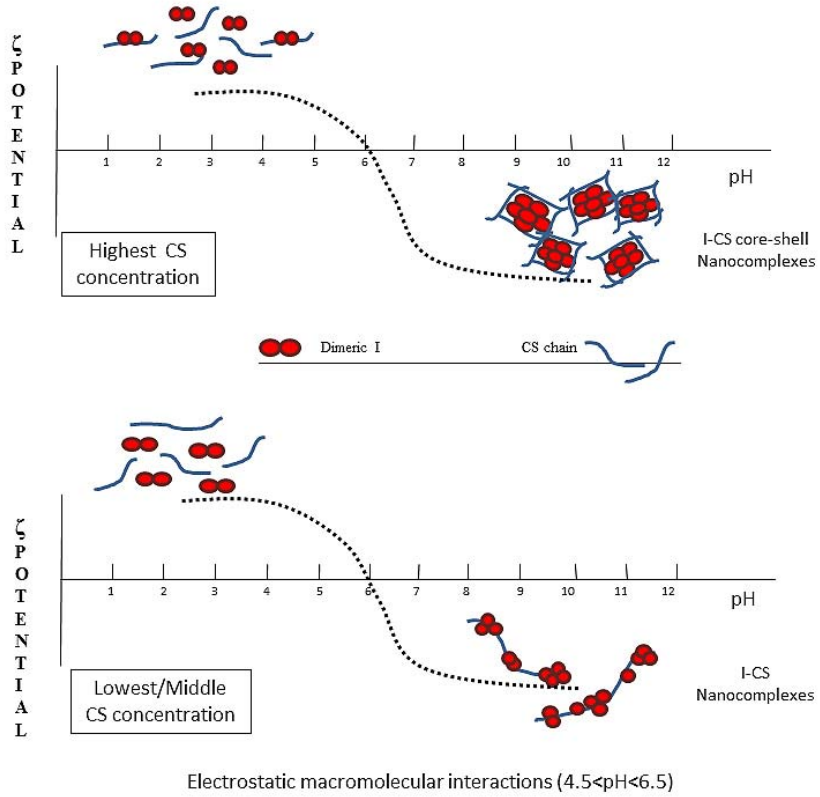

Abstract

The objective of this contribution was to propose a model that would explain the nanocomplexes formation between Human Recombinant Insulin (I) and a polydisperse Chitosan (CS). Such an objective implied exploring I and CS concentration conditions that allowed the formation of complexes with defined and reproducible submicronic dimensions. I-CS complexes were obtained by mixing I and CS solutions at pH 2 and then increasing the pH up to 6 promoting electrostatic interactions between them. Colloidal stages of I and I-CS nano-complexes formation were characterized by dynamic light scattering (DLS), ζ-potential, solutions flow behavior and absorbance measurements. $1 \cdot 10^{-2}$%, w/w, of CS allowed covering completely the surface protein aggregates constituting core–shell nano-structures of 200 nm, with a ζ-potential of 17,5

mV. Solution dynamic viscosity results kept relation with different stages of nano-complexation process. Biological activity of I-CS complexes was studied in 3T3-L1 cultured fibroblast showing a delayed and sustained activity as compared to free insulin. I-CS nano-complexes could be an alternative for developing a new generation of drugs allowing I protection from the hostile conditions of the body and increasing its absorption. These findings have basic and practical impacts as they could be exploited to exert the controlled release of I in therapeutic formulations by using the I-CS nano-complexes.

Keyword: macromolecular assembly, nano-complexes, insulin, chitosan,

1. Introduction

While Insulin (I) is one of the most widely used peptides in the treatment of insulin-dependent patients worldwide, its oral administration has low bioavailability due mainly to the gastric pH and to the enzymatic and physical barriers of the intestinal tract. Intraperitoneal administration, on the other hand, requires I to pass through the peritoneal cavity before reaching the bloodstream [1]. In this context alternative administration routes, are being explored especially those for pediatric uses.

Pulmonary drug delivery is a non-invasive route used for treating a variety of diseases [2]. The lungs provide an extensive alveolar surface area and a dense capillary network that favors drug absorption and enhances drug biodisponibility, while avoiding most barriers associated with systemic administration [3].

Chitosan (CS) is a biodegradable, biocompatible and non-toxic biopolymer that is obtained from chitin after chemical deacetylation process. Chitosan is a cationic copolymer of N-acetyl glucosamine and D-glucosamine, varying in composition, sequence and molecular chain length. The presence of -NH2 and -OH groups gives it interesting chemical and biological properties [4]. With a p*Ka* of approximately 6.5 on the amine groups, CS is positively charged at acidic pH meanwhile it presents negative charges at pH > p*Ka* [5].

The formation of I-CS nano-complexes could be an alternative in the development of a new generation of therapeutic peptides protected from body hostile conditions and with a higher amount of absorption. The controlled release of I could be also modulated with the advantage of enhancing the time interval of bioavailability [6].

The interactions between biological charged macromolecules strongly depend on the type of biopolymer, as well as on the conditions of the medium and its physicochemical

properties (pH, ionic strength, temperature, etc.) [7]. In this context, Mao et al [8] studied the influence of chitosan chain length and ionic strength on I-CS complexation. Chitosan of different chain lengths (all of analytical grade) were considered in the mentioned work. Instead, in the present contribution a new chitosan type, having a polydispersed molecular weight distribution was used. The design of new products has become a key factor in achieving industrial success. Efforts were put by pharmaceutical, cosmetic and food industries focused on reducing the times of manufacturing and in reducing the number of steps when implementing a production system. In this context, the using of our chitosan would reflect a more realistic way to design processes for insulin-chitosan nanoparticles production at industrial levels.

Even although many examples exist regarding single I aggregation processes [9][10] and I-polysaccharides interactions [11][12][13], macromolecular interaction parameters obtained from models application to experimental data (describing the assembling process) are scarce in scientific literature. Several applied analytical techniques allowed us to propose a configuration model for I-CS interactions under the conditions used here. I-CS nano-complexes obtained via electrostatic interactions were characterized in terms of colloidal and flow properties. To complete this contribution, I-CS biological activity was assesed in 3T3-L1 cultured fibroblast.

2. Materials and methods

2.1. Materials

Chitosan was kindly donated by the Microbiology Laboratory of Instituto Nacional de Tecnología Industrial of Mar del Plata, Argentina. In order to use only soluble material, CS was washed previous to its use, as described by Mukhopadhyay [14]. A stock solution

of purified CS 1%, w/w, was prepared, from which subsequent 10-fold serial dilutions were made with 1%, w/w, acetic acid. CS stock solution concentration was 0.2 %, w/w. The viscosity-average molecular weight (MW) of chitosan resulted 300 kDa and was determined according to the Mark-Houwink-Sakurada equation considering $1.81x10^{-3}$ dL g^{-1} and 0.93 values for the K and α constants, respectively [15]. Measurements were done at 25±1°C, by an Ubbelohde viscometer (Thermoscientific, Beverly, MA, USA).

Degree of deacetylation (DD) of CS was determined by elemental analysis. The percentage content of carbon (C) and nitrogen (N) were determined by the CHN EA 1108 Elemental Analyzer (Carlo Erba, New Jersey, USA). Because the deacetylation process has a direct impact on the number of C and N atoms present in the chitosan repeat unity, the following equation, which represents mass ratio between C and N in such unity, can be used to calculate the DD [16]:

$$\frac{C}{N} = \frac{[6 + (1 - DD)x2]x12}{1x14} \qquad (1)$$

Thus, the calculated DD of CS resulted of 72 %.

Chitosan sample had a polydispersity ratio of Mw/Mn = 4.6, where Mw is the weight average molecular weight and Mn is the number average molecular weight.

Recombinant Human I was supplied by Denver Farma Laboratories, Buenos Aires, Argentina. The exact mass of I was dissolved in 20mM HCl solution, pH 2, to give a concentration of 0.4%, w/w.

All other chemicals were of analytical quality. MilliQ water was always used. Biopolymers solutions were kept 24 h at 4 °C to achieve the complete hydration of the molecules previous to their use.

2.2. *Preparation of mixed biopolymers complexes by macromolecular assembly (charge screening method)*

The biopolymer solutions were prepared freshly, filtered through 0.45 mm microfilters (Whatman International Ldt, Maidstone, England) and kept 24 h at 4 °C to achieve the complete hydration of macromolecules. The appropriate volume of each 2X concentrated biopolymer solution was mixed at pH 2, to give the required final concentrations of protein (0.2%, w/w) and polysaccharide in the bulk solution, $1 \cdot 10^{-4}$, $1 \cdot 10^{-3}$ and $1 \cdot 10^{-2}$ %, w/w. I solution was poured into CS under gently magnetic stirring. The mixed solution pH was increased up to 6 by careful addition of Na(OH) (4N) solution, added drop by drop under stirring. At this pH value electrostatic interactions between I and CS would be maximized.

2.3 *Kinetics of aggregation*

Solutions absorbance was registered upon time to study the impact of different CS concentrations in the nano-complexing process kinetics at pH 2 and 6 [17] [18] using a PHERASTAR-FS microplate reader (BMG LabTech, Ortenberg, Germany). Absorbance of I solution was also registered as a control. Data was acquired at λ=500nm, away from I and also CS intensities peaks [19]. All measurements were performed at 25 °C; 200 µl of each solution was poured into each well. Then, kinetic parameters were obtained as proposed by Stirpe *et al* [20].

2.4 *Dynamic Light Scattering (DLS) and ζ – potential*

Particle size distribution and its derived parameter, main peaks, and ζ - potential measurements were carried out using a Zetasizer Nano-Zs particle analyzer (Malvern Instruments, Worcestershire, UK). All samples were analyzed with an angle of 173°, at 25°C. Each measure consisted in 10 runs. Particle size distribution was obtained as indicated by Pérez *et al.* [21]. The intensity distribution is determined using a multi exponential function (CONTIN) to fit the correlation data. In this type of analysis, the presence of more than one family of particle sizes is taken into consideration. These multiexponential algorithms, for which there is no standard and which generally vary from manufacturer to manufacturer, will generate an intensity distribution and, using the Mie theory, a distribution normalized for the volume of the scattering particles [22] Volume size distribution was considered to determine the relative importance of each peak. The following constants were used for measurements: RI: 1.333 for ultrapure water; which was the dispersant, dielectric constant: 78.5 , viscosity: 0.8872 cp, equilibration time was always 180 s .

ζ -potential was evaluated from the electrophoretic mobility of the particles, at 25 °C. The conversion of the measured electrophoretic mobility data into ζ -potential was done using Henry's equation [23] [21]. Disposable capillary cells were used to perform these experiments (DTS1060, Malvern Instruments, Worcestershire, UK).

2.5 *Flow behavior*

Rheological characterization of I, CS and I-CS solutions was carried out using an Anton Paar MCR 301 (Physica MCR 301, Anton Paar, Germany) stress controlled rheometer. Flow curves were obtained at 25 ºC using cone plate geometry, CP50 (50 mm diameter, 1º cone angle and 0.099 mm gap) and shear rate varied from 0.01 to 1000 s^{-1}. 560 µL of each sample were placed in the determination platform of the instrument. Tests were done

in automatic mode to ensure that the steady state at each shear rate was reached. Experimental data were fitted by applying the following Power Law model:

$$\tau = K\dot{\gamma}^{n} \qquad (2)$$

Where τ is the shear stress (Pa), $\dot{\gamma}$ is the shear rate (s^{-1}), *K* is the consistency coefficient (Pa.s), which is commonly homologated with the viscosity and *n* (dimensionless) is the flow behavior index [24].

2.6 *Cell culture and Western blotting*

3T3-L1 fibroblasts cells were obtained from ATCC® CRL-1658™. Cells were grown in Dulbecco's modified Eagle's medium (DMEM) supplemented with 10% fetal bovine serum (FBS) and penicillin/streptomycin (50 U/ml; 50 µg/ml) (all Gibco; Thermo Fisher Scientific, Inc.). Cultures were maintained in a humidified incubator at 37°C with 5% CO_2 and 95% air.

Western blots were performed according to standard procedures. Briefly, $5 \cdot 10^4$ cells were seeded in plates of 6 wells during 48 h. until 70% of confluence. 3T3-L1 were serum starved for 4 h. and treated with I, $6 \cdot 10^{-5}$ % w/w or I-CS complexes containing an equivalent I amount for 0, 0.5, 2, 30 and 120 min. Cells were immediately scraped in cracking solution (Tris-HCl 200 mM, SDS 8%, Bromophenol Blue 0.4%, Glycerol 40% and β-mercaptoethanol 400 mM) with proteases inhibitors (P8340 SIGMA, St Louis, USA) and phosphatases inhibitors (NaF 50 mM, Sodium Orthovanadate 2mM and β-glycerolphosphate 10 mM). Lysates were separated on 10 % SDS- polyacrylamide gel and transfered onto a PVDF membrane (Amersham Hybond GE Healthcare Life

Sciences, Germany). Blotting efficiency was verified by staining the membrane with Ponceau Red. Membranes were blocked with 5% BSA in TBS (150 mM NaCl in 50 mM Tris-HCl buffer pH 8) for 1 h. and then incubated overnight at 4ºC with rabbit anti-P-Akt S473 (Cell Signaling, USA). Rabbit IgG-HRP (Santa Cruz, CA, USA) was used to detect Immunoreactive bands by chemiluminescence, with ECL Prime Western Blotting Detection Reagents RPN 2232 (Amersham GE Healthcare, UK).

3. Results and discussion

3.1 Intermacromolecular association kinetics in mixed solutions

Protein aggregation depends on several parameters including time, pH, concentration and solvent properties [25] [26]. In this context, self-association of I molecules into dimers, hexamers, and macromolecular aggregates has been reported before [27]. On the other hand, CS aggregation starts to occur at concentrations as high as 0.1%, w/w, as reported by Phillipova [28], well above the ones used in this work. Absorbance measurements (i.e. scattering or turbidity) were used here to understand the kinetics of aggregation of both species and how CS influences I aggregation meanwhile nano-complexes formation ocurred. Turbidimetric studies as applied to protein-polysaccharide systems were based on the fact that turbidity is proportional to both size and concentration of the particles formed [29].

Fig. 1 shows the absorbance as a function of time which was registered for three different concentrations of pure CS, at pH 2 and pH 6 (Fig. 1a); pure I and I-CS mixed solutions at pH2 (Fig. 1b) and at pH 6 (Fig. 1c). Single polysaccharide did not register remarkable changes in absorbance at the considered pH values, indicating the absence of scattering

(Fig. 1a), as demonstrated by the insignificant changes observed in the "y" axis. Figure 1b shows the results concerning to mixed systems at pH 2 which corresponded to the pH value at which biopolymers solutions were mixed. Single I and CS solutions did not show absorbance change in the considered frame of time indicating co-solubility of biopolymers. The electrostatic interactions between both biopolymers would be minimized meanwhile the repulsive forces between the macromolecules would be maximized. The protein has positive charge as its isoelectric point (pI) was reported to be ~ 5.4 [30]. On the other hand, the polysaccharide is positively charged at pH<6.5 due to the protonation of the amino groups [14].

Absorbance was also registered as a function of time at pH 6 for I and I-CS (Fig. 1c). Under these conditions nano-complexation process would be favored via electrostatic interactions. Insulin presented negative and CS positive surface charges, respectively. The curve for single I was included as a reference for the analysis of mixed systems behavior. No remarkable changes were observed in the absorbance for pure I as time elapsed. This behavior could obey to the fact that the protein aggregation process could occur at a limited scale (small aggregates) or at a low formation rate. Single protein aggregation would not be impeded as I is near to its pI value and the protein concentration was above its critical aggregation concentration [31]. Therefore, the formed protein aggregates would not have a size big enough to scatter light.

I-CS mixed systems showed an initial low absorbance value that started to increase over time. Changes in absorbance could be attributed to the scattering due to protein solution turbidity increase [20]. Turbidity, a measure of the extension of I aggregates formation induced by the presence of CS or due to the intermacromolecular arrangement, variated inversely with the polysaccharide concentration. Similar trends concerning to turbidity behavior were reported by Mao et al [8]. CS concentration influenced the aggregation

state of the protein, i.e. aggregates characteristics such as size and shape, and the rate of formation. The time needed for increasing turbidity varied with the amount of added polysaccharide. Protein aggregation and macromolecular interactions with CS requires a special thermodynamic state previously acquired by the protein molecules for this process to take place [19]. This protein state, which seems to be a general rule, was reported for myoglobin [32], BSA [33], β-lactoglobulin [34], whey protein concentrates and isolates and ovoalbumin [35].

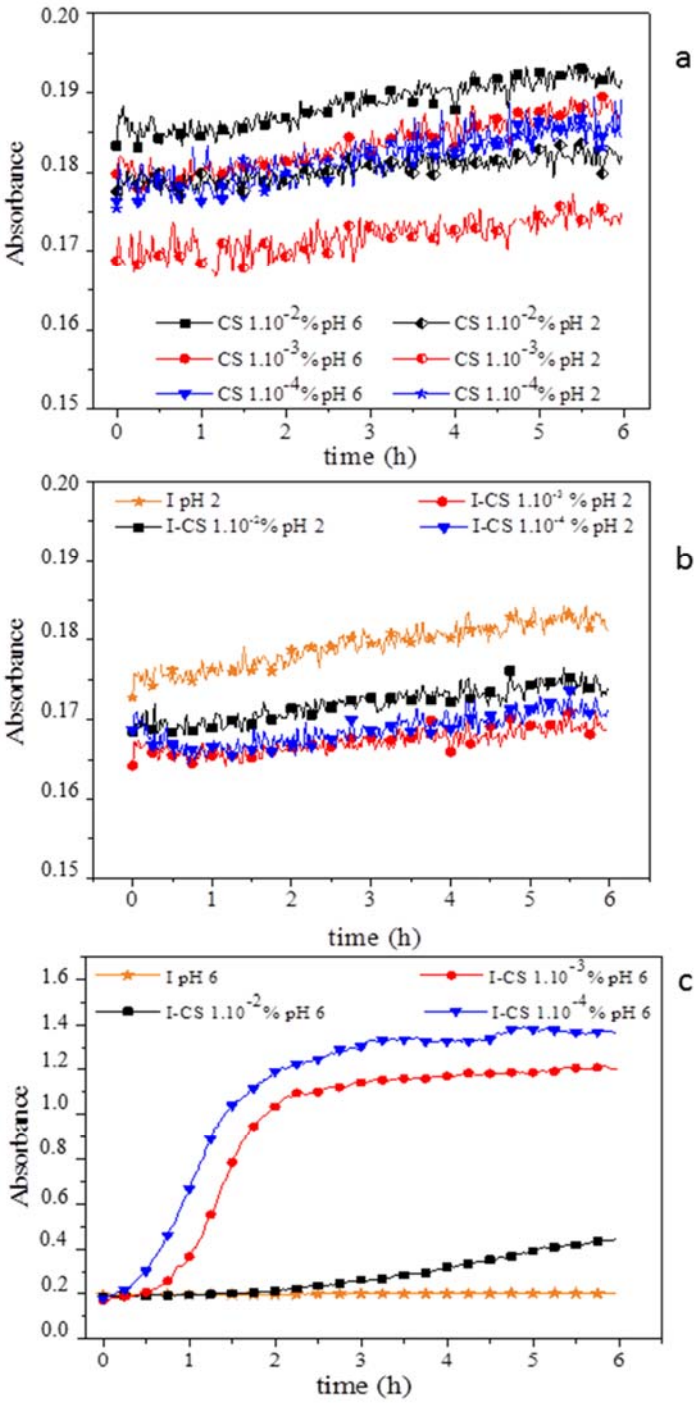

Fig. 1**.** Time dependence of the absorbance at 500 nm for CS solutions registered (a) pH 2 and 6 (b) and I-CS mixed solutions at pH 2 and (c) pH 6. Pure protein solution concentration, 0.2 %, w/w, was monitored for comparison. CS concentrations in mixed solutions were $1 \cdot 10^{-4}$, $1 \cdot 10^{-3}$ and $1 \cdot 10^{-2}$%, w/w. Temperature: 25 °C.

The kinetics model application to experimental absorbance *vs* time data allowed determining the α (s^{-1}) and β (dimensionless) parameters, which corresponded respectively to the rate and the order of spontaneous aggregate formation [20]. Equation (3) corresponds to the function used to fit the experimental data for obtaining the mentioned parameters:

$$y = y_0 + c.e^{-(\alpha.t)^{\beta}} \qquad (3)$$

Thus, a faster aggregates formation was observed for those systems containing the lowest CS concentration ($1 \cdot 10^{-3}$ and $1 \cdot 10^{-4}$ %, w/w) as indicated by the α values obtained from the model application (Table 1).

On the other hand, α values corresponding to pure I and that of I-CS $1 \cdot 10^{-2}$ %, w/w, resulted lower than the former ones. The α value for pure protein was in line with the hypothesis explained before that single protein aggregation occurred at a lower rate or was non extensive, as manifested by the absorbance *vs* time curve.

Table 1

Sample	α(s^{-1})*	β*	R^2
I	not applicable	not applicable	
I-CS $1 \cdot 10^{-2}$%	0.24 ± 0.06^{a}	4.1 ± 0.9^{a}	0,99
I-CS $1 \cdot 10^{-3}$%	0.65 ± 0.09^{b}	3.2 ± 0.7^{a}	0,99
I-CS $1 \cdot 10^{-4}$%	0.76 ± 0.16^{b}	2.1 ± 0.8^{a}	0,98

Kinetic parameters describing intermacromolecular association process as determined by fitting the absorbance curves for single Insulin and I-CS mixed solutions. Samples were analyzed at pH6.

*mean±SD of replicates corresponding to three independently prepared samples solution.

A lag phase at the highest CS concentration ($1 \cdot 10^{-2}$%, w/w) suggested that the polysaccharide had impact on I, which was visualized as a higher amount of time needed for the aggregation process to start. The long interval time observed for I-CS $1 \cdot 10^{-2}$ %, could be attributed to the existence of sequential or multiple stages during global biopolymer association. Although absorbance showed a sigmoidal-like behavior for all mixtures, reaching a plateau after 2 hours approximately, I-CS $1 \cdot 10^{-2}$%, w/w mixed system described a remarkable lag phase. Absorbance remained constant before its enhancement, and a plateau was reached after biopolymers association process became stable. This lag time was attributed to the time needed by the protein molecules to acquire the state that favors the association process, which variated according to the amount of CS in the solution bosom. In fact, protein-to-polysaccharide ratio is crucial to control the charge balance between interacting biopolymers [36]. For a specific protein–polysaccharide pair, there is an optimal ratio for which electrostatic interactions reach equilibrium between repulsive and associative interactions, allowing the formation of different intermacromolecular or complexing patterns. The polysaccharide, being a polyelectrolyte able to cover I aggregates surface at the highest bulk concentration studied, would be increasing the electrostatic repulsion between the complexes once formed and concomitantly decreasing the probability of association.

β parameter completed the analysis of data fitted with the kinetic model occurring with I at different CS concentrations. The protein aggregates formation process becomes more cooperative and complex involving the formation of intermediates as indicated by the lower values of β (Table 1) [34][37]. Higher β values indicate that more intermediate species were formed as the I aggregation proceeded as evidenced in I-CS systems,

containing $1 \cdot 10^{-2}$ % w/w of CS. Therefore it could be concluded that CS amount would be modulating protein aggregation and the intermolecular association as well.

It can be observed that the rate of absorbance increase is inversely proportional to CS´s concentration. This result is a manifestation of a decrease in the *bridging-flocculation* phenomenon, in analogy to the term used in emulsion science. Briefly, the long polysaccharide chains are able to bind more than one protein aggregate, forming protein molecular clusters. Thus, each cluster is formed by charge neutralization and bridging effects. This effect is most pronounced at lower polysaccharide concentrations where protein aggregates surfaces are only partially covered. This finding is in line with the results published in the pioneer paper of Mao et al [8] and those obtained in a more recent paper by Sogias et al. [19], who attributed the changes in absorbance of mucin solutions to the formation of biggest clusters at low CS concentrations. In other words, smaller nano-complexes were formed at lower I/CS ratio.

Accordingly, the results presented hereinafter concerning to I-CS mixed systems were derived from 3 h aged solutions after mixing and pH adjustment to 6. This time was considered enough to reach a plateau for I-CS intermacromolecular association as determined by turbidity measurements.

3.2. Particle Size characterization of mixed biopolymers complexes

A study of size distribution was performed by DLS, which is based on the Brownian motion of particles. Fig. 2a shows the volume size distributions for I at pH 2 and 6. This protein displayed a monomodal distribution at both pH values. At the lower one, pH 2, the peak was broadening from 1.4 to 2.1 nm with a maximum at 1.8 nm. The area under the peak includes I monomers, and structures larger than dimers as well. Particle size

distribution of I was displaced to higher sizes at pH 6. Particle size distribution, being also monomodal, manifested a maximum value at 2.6 nm with 2 and 5 nm peak limits. At this matter, it can be pointed out that self-association state of a protein can be influenced by intrinsic solution properties, such as the protein concentration, pH and the ionic strength, or extrinsic conditions as temperature, radiations, electric power, etc. Table 2 resumes the parameters derived from particle size distribution analysis. Thus, at pH 2, the measured diameters for the protein coincided with dimeric quaternary structures. The molecular weight was estimated from empirically determined size *vs.* protein mass relationships. At pH 6, the measured diameters by the same methodology were consistent with the hexameric forms of the protein, in coincidence with the literature [38].

In respect to mixed systems, a subtle trend was observed, as CS concentration increases, the maximum peak decreases and the particle size distribution tended to be monomodal as well. Thus, the measured diameters for I-CS system containing $1 \cdot 10^{-2}$% w/w, of CS, are consistent with a monomeric structure of I. At pH 2 the electrostatic interactions are minimized given by the protein pI and the CS p*Ka* [39] [18].

The polysaccharide may induce the modification of insulin native structure and even trigger the proteins aggregation, via molecular interactions other than the electrostatics (hydrophobics, Van der Waal forces, etc) [40]. The non-polar regions of the protein surface could interact with the less polar region of the polysaccharide, modulating the possibility of protein association or oligomers dissociation.

Table 2

	pH 2		pH 6
MONOMODAL DISTRIBUTION		MULTIMODAL DISTRIBUTION	
Sample	**Peak (nm)***	**Sample**	**Peaks (nm)***
I	2.0 ±0.09	I	2.6 ± 0.02
I-CS $1 \cdot 10^{-2}$%	1.5 ±0.04	I-CS $1 \cdot 10^{-2}$%	95, 129
I-CS $1 \cdot 10^{-3}$%	1.7 ±0.03	I-CS $1 \cdot 10^{-3}$%	92, 130, 188
I-CS $1 \cdot 10^{-4}$%	1.7 ±0.06	I-CS $1 \cdot 10^{-4}$%	196, 328

Particle size parameters from volume size distribution analysis, obtained from DLS measurements for single Insulin and I-CS mixed solutions at pH 2 and 6.
*mean±SD of replicates corresponding to readings of three independently prepared samples solutions. Data were obtained at 25°C.

At pH 6, I-CS systems showed a multimodal behavior in size distributions (Fig. 2c). As can be seen, the entire distribution displaced to lower sizes upon increasing CS concentrations. The particle size distribution of I-CS system with CS $1 \cdot 10^{-4}$%, w/w, manifested two peaks, the first at 196 and the second at 328 nm (Table 2). Mixed solution with CS $1 \cdot 10^{-3}$ %, w/w, presented a multimodal behavior with peaks placed at 92, 130 and 188 nm respectively. It is important to note the behavior described by mixed solution with CS $1 \cdot 10^{-2}$ %, w/w, that had one main peak observed at 129 and a shoulder located at lower sizes, 95 nm. The remarkable change observed for I-CS mixed solutions at pH 6 in comparison with the behavior observed at pH 2, could obey to two reasons. First of all, the electrostatic interactions could be maximized and complexation would occur as both biopolymers had opposite surface electrical charge at this pH. The second reason has a connection with relative biopolymer concentrations. In general terms, it could be said that particle size decreased as CS bulk concentration increased. Such an effect was explained as a decrease in the *bridging-flocculation* effect, which was previously explained. In line with the results presented here, Sogias [19] reported that mucin aggregation decreased as

CS concentration increased, and that was related to a subsequent protein disaggregation caused by the excess of cationic polymer in solution and further complexation. To sum up, particle size distribution results were in line with those found by absorbance studies in section 3.1.

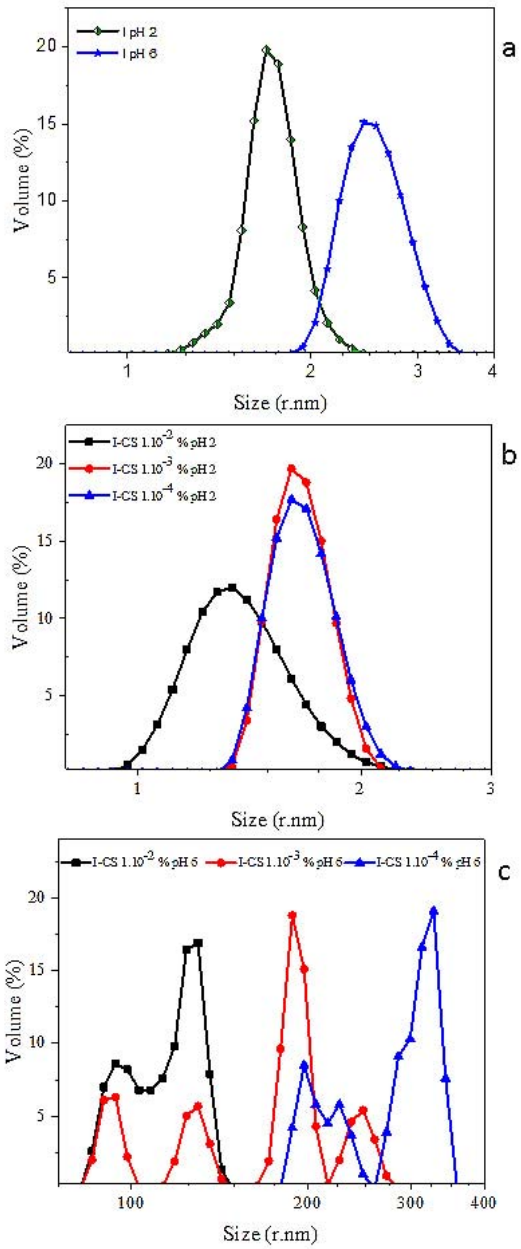

Fig. 2. Volume particle size distribution (based on DLS data) of (a) Insulin at pH 2 and pH 6. (b) Curves obtained for I-CS nano-complexes at pH2 (c) and pH 6. Pure protein solution, 0.2 %, w/w, was monitored

for comparison. CS concentrations in mixed solutions were $1 \cdot 10^{-4}$, $1 \cdot 10^{-3}$ and $1 \cdot 10^{-2}$ %, w/w. Temperature for DLS measurements was 25 °C.

3.3. *Mixed biopolymers complexes characterization*

Single chemical species previously characterized in terms of size were analyzed comparatively in terms of surface charge. Fig. 3 shows the ζ-potential values for single biopolymers aqueous solutions as a function of pH. It can be seen that ζ -potential varied between 25 mV at pH 2 and -35 mV at pH 6 for pure I, with a point of zero charge around pH 5, in coincidence with the reported pI value [41]. Surface electrical charge of CS solutions variated between 6 mV at pH<6 (lower than the amine groups p*Ka*) and -20 mV at pH>7 (higher than the amine groups p*Ka*). The global surface charge corresponding to zero for CS was around pH 6.5. The superimposition of curves for I and CS (Fig. 3), allowed the establishment of the optimum pH range that maximizes the occurrence of electrostatic interactions between I and CS molecules, which occurred between 5.0 and 6.5. Interaction pH range is pointed out by the shaded gray zone in Fig. 3. Thus, pH 6.0 was selected due to practical benefits since it was more easily adjusted. As the pH was increased, from 2 to 6, the number of anionic groups on the protein also increased, inducing the electrostatic attraction with the CS cationic groups. In practical terms, the electrostatic complexation between CS and I generated nano-complexes, whose dimensions clearly fell into the so called submicronic scale (<1 μm) [42].

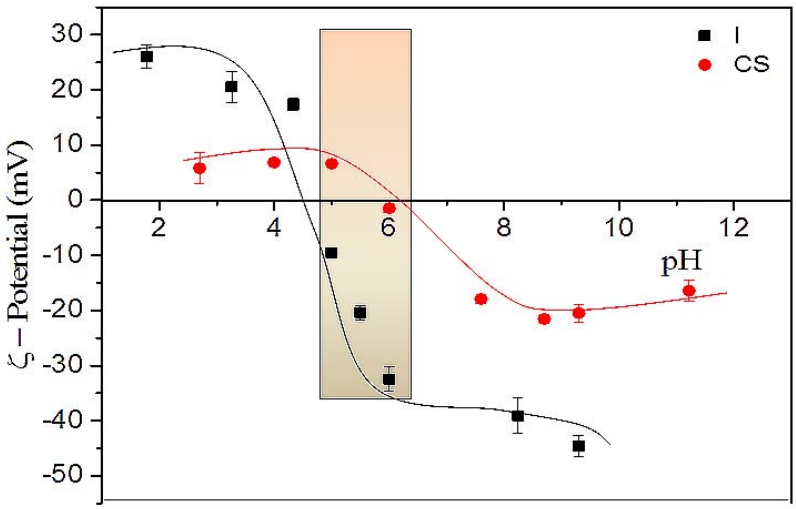

Fig. 3. Influence of pH on the electrical charge (ζ-potential) of solutions containing Insulin and Chitosan $1 \cdot 10^{-3}$%, w/w. Shaded zone in the graph indicates the highest probability for the electrostatic interactions between molecules. Temperature: 25 °C.

.

ζ-potential provides indicative evidence towards the nature of surface charges assuming that the predominant ions in the electric double layer up to the slipping plane are similar (positive/negative) compared to the surface of the particle itself. The practical way to confirm the nature as well as to determine charge density on nanoparticles is to titrate it with known amounts of ions or polyelectrolytes [43]. The results obtained for surface charge titration are shown in Fig. 4. ζ-potential values were analyzed at pH 6 for mixed systems, in which protein concentration was kept constant, 0.2%, w/w, as CS concentrations increased. It is shown that both I and I-CS mixed solutions had values placed between -35 mV at 0% w/w, and 20 mV at 0.1% of CS, respectively. This type of

plots reveals the gradual increase in the particle surface charge with interacting CS concentration increase. The existence of surface charges on the complexes assures colloidal stability which prevents the formed nano-complexes for further aggregation.

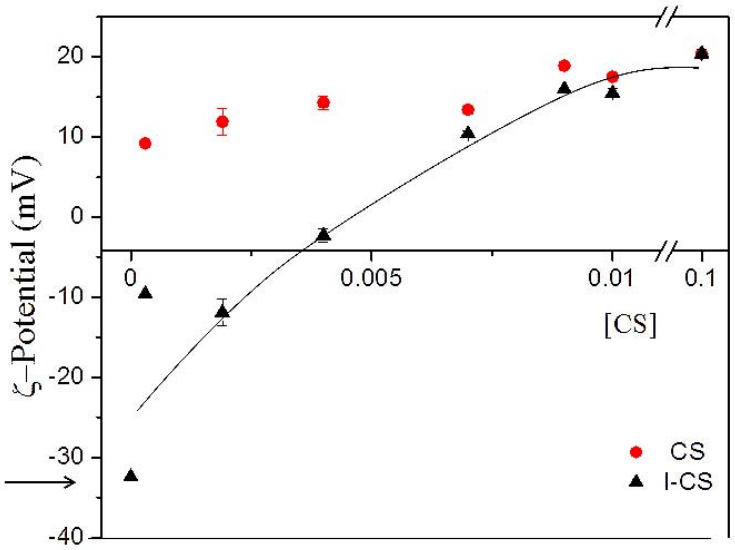

Fig. 4. ζ -potential values of Insulin, 0.2%, w/w, with variable concentration of chitosan (I-CS), compared with samples containing pure chitosan, at pH 6. Measurements were perfomed after 3 hours of I-CS mixed solution preparation. Black arrow indicates pure Insulin ζ-potential. Temperature: 25 °C.

Associative interactions between opposite charged I and CS have a profound impact on determining the structure of nano-complexes, granting their physical stability. In other words, associative interactions prevent the complexed biopolymers from dissociation and imparting functionality during storage and the passage through the epithelium in delivery systems [44].

Protein–polysaccharide associative interactions allowed designing colloidal particles. It was claimed that steric effect and the thickness and porosity of the polysaccharide layer also contributes to colloidal stability of complexes besides the electrical characteristics of the adsorbed layer [45]. I-CS would not be the exception. As seen in Fig. 4, mixed solution up to 0.003% w/w of CS, manifested ζ-potential values significantly more negative than CS's alone. Mixed systems acquired positives values at concentrations of CS equal to 0.005%, w/w, or higher, drawing on closer to the values found for pure CS solution. At the CS concentration ≥ 0.1%, w/w, the complexes were found to approach to their maximal ζ-potential value, which was also very close to the value for free CS. In our experiments no further charge reversal was observed when the CS concentration increased. Surface charge saturation could indicate that the formed nano-complexes would have a core-shell type nanostructure, with insulin forming the core and CS the shell [46], respectively.

3.5. Rheological properties of I-CS solutions

Polymers solutions viscosity must be characterized for systems with applications in the pharmaceutical and biomedical fields, such as in this case. The combination of two biopolymers determines the mixed solution viscosity. In turn, two biopolymer solutions mixing could also lead to subsequent processing difficulties, modifying degradability, and availability of functional groups in the crosslinked polymer or even to a potential increase in cytotoxicity [47]. Rheological properties of I-CS nano-complexes solutions were studied in comparison with single I solution, Fig. 5a displays the flow curves for these systems, or shear stress *vs* shear rate curves. These curves represent the real experimental data obtained from rheological determinations. It can be seen that the shear stress

increased with shear rate in all cases into the studied shear rate domain. Fig. 5b shows the apparent viscosity variation with shear rate, from which the character of flow can be obtained. Thus, it was observed that I and I-CS $1 \cdot 10^{-2}$ %, w/w exhibited a characteristic non-Newtonian behavior being more viscous than the remaining mixtures up to 200 s^{-1}. I-CS mixtures with $1 \cdot 10^{-3}$ and $1 \cdot 10^{-4}$ %, w/w of CS, manifested a similar behavior between them (Fig. 5b). This result indicates that the rheological behavior of the solution resembled the one of the protein, at the highest polysaccharide concentrations (CS $1 \cdot 10^{-2}$%, w/w). In other words, the behavior within the rheometer was very similar, for both I and I-CS $1 \cdot 10^{-2}$%, where single individual particles, with no entanglement, were detected.

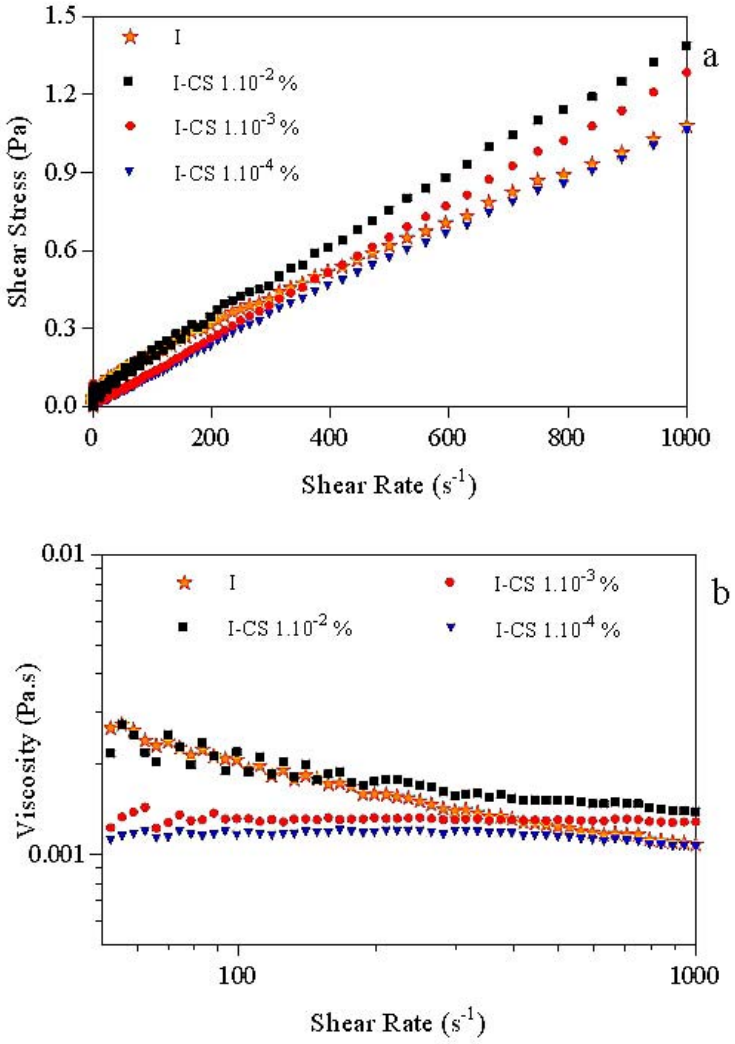

Fig. 5. Flow curves for (a) I-CS mixed solutions and (b) viscosity, registered at pH 6. Pure protein solution concentration, 0.2 %, w/w, was included for comparison. CS concentrations in mixed solutions were $1 \cdot 10^{-4}$, $1 \cdot 10^{-3}$ and $1 \cdot 10^{-2}$%, w/w. Temperature of measurements 25 °C.

To obtain quantitative parameters from the rheological experimental data, Power Law model was used to describe the flow curves. The corresponding parameters obtained from the model are shown in Table 3. The high correlation coefficients obtained ($0.988<R^2<0.998$) indicate that the model appropriately fitted the experimental data.

It can be observed that an increase of the polysaccharide concentration provoked a decrease in *K* parameter in comparison to pure I solution. Meanwhile, *K* resulted lower when CS was at $1 \cdot 10^{-3}$ and $1 \cdot 10^{-4}$%, w/w. Lower *K* values than those of pure I aqueous solution would confirm biopolymers co-solubility enhancement and the formation of less entangled macromolecular rearrangement in the solution bosom. Single I and I-CS $1 \cdot 10^{-2}$%, w/w, presented the highest K values. In terms of surface charges, nano-complexes would stay more separated due to higher repulsion as the surface of protein was completely covered by CS. The flow behavior $n = 1$ indicates a Newtonian fluid and $n < 1$ represents a shear thinning fluid because the slope of the curve decreased as shear rate increased [48]. At this respect, two different trends were defined, one for pure I solution, which was shear thinning, and the other for I-CS mixed systems with *n* values between 0.8 and 1. The latter clearly denotes a tendency towards a Newtonian behavior, related to the cosolubility increase as the CS concentration decreased as reported.

Table 3

Sample	Power Law parameters		
	$K.10^3$ (mPa.s^n)*	n*	R^2
I	8.451 ± 0.505^a	0.695 ± 0.007^a	0.994
I-CS $1\cdot10^{-2}$ %	4.940 ± 0.495^b	0.813 ± 0.012^b	0.988
I-CS $1\cdot10^{-3}$ %	1.590 ± 0.289^c	0.969 ± 0.028^c	0.992
I-CS $1\cdot10^{-4}$ %	1.764 ± 0.096^c	0.928 ± 0.006^c	0.998

Consistency index (*K*), and flow behavior index (n) for single Insulin and I-CS mixed solutions (pH 6),derived from Power Law application.
*mean±SD of replicates corresponding to readings of three independently prepared samples solutions. Data were obtained at 25°C. Different letters indicate statistically significative differences at $p<0.05$.

The ANOVA test results (Table 3) indicate that the four solutions can be divided into three homogeneous groups: single I, I-CS $1\cdot10^{-2}$ % and I-CS for $1\cdot10^{-3}$ and $1\cdot10^{-4}$ %.

Thus, three stages can be characterized from the rheological experimental data at pH 6, in accordance to particle size, ζ -potential and absorbance measurements. The first, concerning to the single I solution, which has the highest *K* and the lowest *n* values, presented a negative surface charge, making the protein highly soluble by virtue of electrostatic repulsion between molecules. In general terms, a lower viscosity was observed for mixed systems evidencing the polysaccharide influence. Such a decrease was stronger as the CS concentration increased, with the concomitant trend to a non-Newtonian behavior at $1\cdot10^{-2}$%, w/w of the polysaccharide. Thus, the decrease in viscosity could be explained by the adsorption of cationic chitosan on the surface of negatively charged insulin. At pH 6 biopolymers carry opposite charges and complexation process occurred with particular features. When chitosan concentration was low, there was insufficient CS available to coat the anionic protein aggregates and clusters of higher sizes were formed (*bridging- flocculation*) which contributed to a slight

decrease of viscosity. At this respect Bohidar et al (2005)[49] described such a behavior in terms of soluble protein-polyelectrolyte complexes. Interactions in solution bosom between such complexes were presumed to provide cross-links which could be stable in time and modulating flow properties.

On the other hand, c*ore-shell* nano-complexes were formed in mixed solutions, with CS concentrations above a critical one (0.01 %, w/w). The attractive forces between Insulin and cationic chitosan promoted the formation of microphases rich in nano-complexes, that increased the viscosity of the system. This behavior was also explained by Bohindar et al (2005) referring to the presence of complex rich domains, i.e. core-shell, more viscous, leading to the formation of complex-poor microphases, which would be more fluid [48].

3.6 Association model

In function of the obtained results we proposed a configuration model for insulin and chitosan assembling via macromolecular interactions (Fig 6). The phenomena occurring from single I molecules as the CS concentration increases can be divided into three stages at pH 6.

Insulin pI determines the existence of a turning point. At pH lower than 5.5, I dimer formation was observed regardless CS concentration, as determined by DLS [49], ζ-potential and absorbance measurements. This phenomenon occurred at a slow rate and was less cooperative than systems constituted by higher amounts of CS as confirmed by the parameters obtained from turbidity data fitting.

At pH higher than 5.5, when the protein has a negative surface charge, two scenarios were observed: core-shell complexes were formed at the highest CS concentration (1·10-2%, w/w) (Fig. 6a). This solution presented a non-Newtonian behavior and the highest

apparent viscosity of the three mixtures. Regarding to the lowest CS concentrations ($1 \cdot 10^{-4}$ and $1 \cdot 10^{-3}$%, w/w), bridging-flocculation process took place, resulting in larger clusters, as indicated by DLS (Fig. 6b). This process occurred at higher rate with fewer molecular intermediates forms as indicated by α and β values obtained from fitting the absorbance vs time data. Lower values of apparent viscosity would indicate the formation of weakly entangled macromolecular rearrangements.

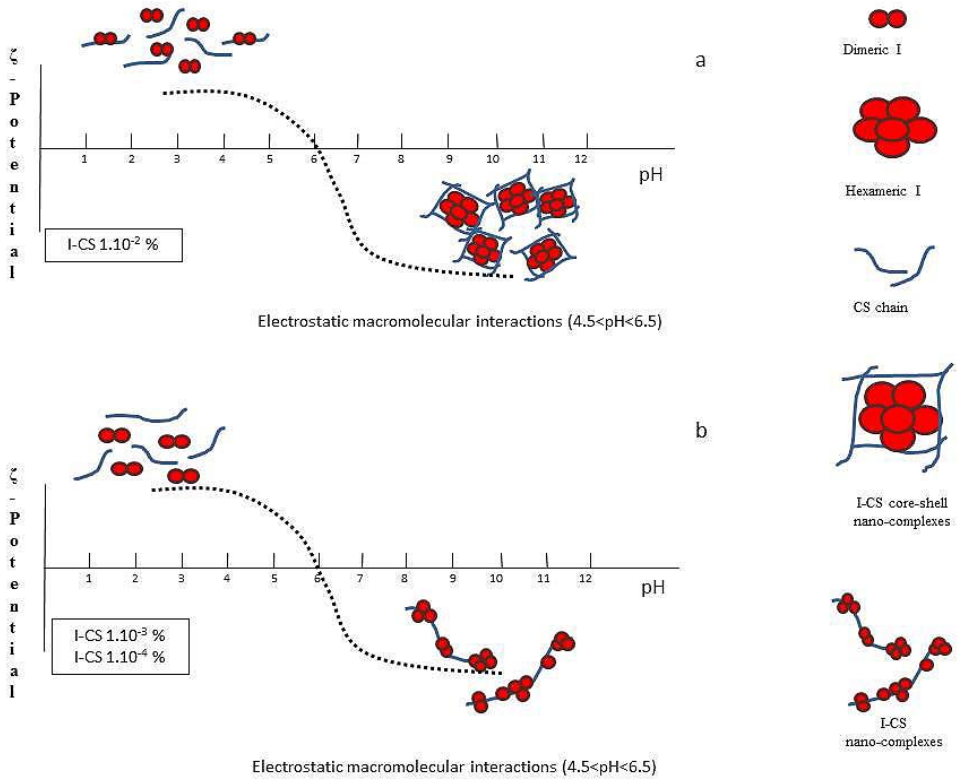

Fig. 6. Scheme showing the configuration events occurring during I-CS nano-complexation as modulated by the pH of mixed solution and CS concentration. (a) CS concentration 1·10-2% with no association between I dimers and CS, at pH<pI of I. Core-shell nanostructures at pH>pI. (b) CS concentration<1·10-2%. No association between I dimers and CS, at pH<pI I-CS systems. Nano-complexes of different structures were formed by macromolecular entanglements at pH>pI.

3.6 Activity in cultured cells

In order to evaluate the biological activity of *core-shell* I-CS nano-complexes (I completely covered by $1 \cdot 10^{-2}$% CS), we measured the activation of the insulin-induced signaling pathway in 3T3-L1 fibroblasts. This is a well-established I responding preadipocyte model [50]. Activation of the insulin receptor at the cell membrane rapidly recruits and activates by phosphorylation IRS-1 and AKT leading to the translocation of the glucose transporter and the activation of the metabolic response[51] .Following activation, receptors are internalized into endosomes were they could be recycled or transported to lysosomes for degradation [52]. To quantify the dynamics of the I pathway activation by I-CS, changes in phosphorylated AKT levels,, were measured by Western blot at different times after ligand induction . As shown in Fig. 7a, I-CS stimulation displayed a delayed and sustained activation of AKT as compared to single I. This experimental result confirms that the structural and functional stability of Insulin and its release from the nano-complexes allows a sustained stimulation of the I signaling in 3T3-L1 cells.

The covering of I by a shell of CS in nano-complexes would explain the delayed activation of its cellular response, with no instantaneous access to cell receptors. Free I molecules binds to its receptor and the activated ligand-receptor complex is fully internalized within 120 min [52]. On the other hand, the sustained activation exterted by I-CS core-shell nano-complexes upon time indicates I releasing from the nano-complexes in a time dependent manner. Fig. 7b represents the quantification of AKT activation over time by I or I-CS stimulation. A clear difference in their activation profile was observed. While I stimulated activation reached a maximum after 10 min and had a further decrease, I-CS showed a sustained activity after 120 min. This finding has practical

impact as this property could be exploited to exert the controlled release of I in therapeutic formulations by using the I-CS nano-complexes.

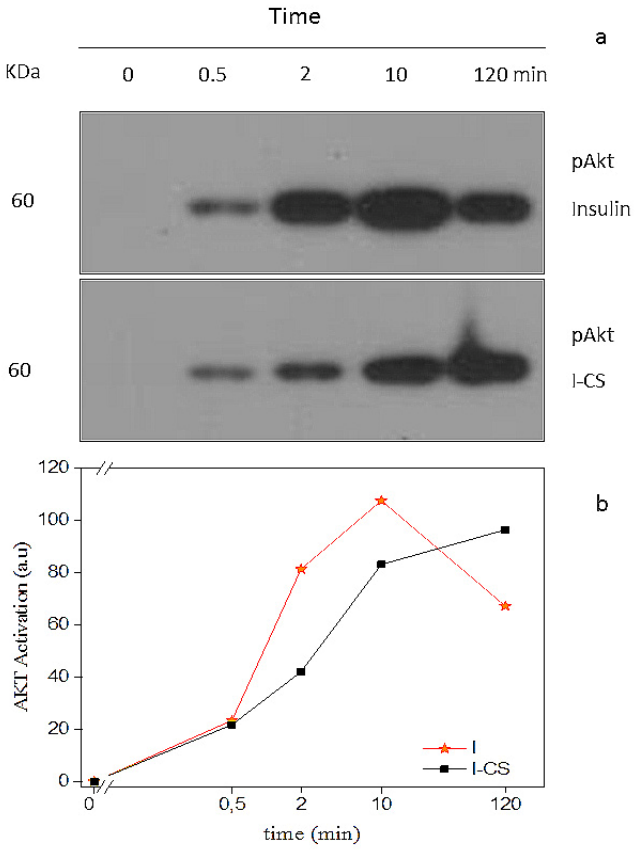

Fig. 7. (a) Western blot showing changes in phosphorylated AKT levels after I or core-shell I-CS (1·10-2% CS) stimulation assayed in 3T3-L1 fibroblasts upon time. (b) Quantification of AKT activation over time showing a sustained increase for I-CS activation after two hours of stimulation.

Conclusions

Insulin-Chitosan nano-complexes were designed by applying the macromolecular assembling principle. The CS solution concentration for complete protein aggregates surface coverage was determined as $1 \cdot 10^{-2}$%, w/w, i.e. constituting core-shell type nano-

complexes. The interactions between both biopolymers were modulated by the pH of the solution. Hydrodynamic and colloidal interactions were evaluated by light scattering technique. ζ-potential determinations made possible to find the electrostatic interaction zone between these macromolecules. This approach has also resulted useful to determine the I surface coverage by CS. Flow curves properties reflected the biopolymers association and the shape pattern of nano-complexes. Mathematical models application to the experimental data allowed obtaining parameters that described the nano-complexation process, i.e. the kinetics parameters of nano-complexes formation under the conditions here considered.

I-CS nano-complexes could be an alternative in the development of a new generation of pharmaceuticals for protein protection from the hostile conditions of the body, increasing its absorption and exerting the controlled release as demonstrated by the biological activity assay. Furthermore, the nano-complexes generated according to this configuration could be the starting point for new drug designs aimed at new administration routes, such as pulmonary, relevant for pediatric uses.

Acknowledgments

This research was supported by Projects 20020150100079BA, Universidad de Buenos Aires, Universidad Nacional de Luján, ANPCyT (PICT2013-1985; PICT-2014-1402 and PICT-2015-3866), CONICET of Argentina and Comisión de Investigaciones Científicas of the Province of Buenos Aires (CIC). The authors also thank to Lic. Belén Bonecco of INTI, Mar del Plata and Denver Farma of Argentina.

Bibliography

[1] P. Fonte, F. Araújo, C. Silva, C. Pereira, S. Reis, H. a. Santos, B. Sarmento, Polymer-based nanoparticles for oral insulin delivery: Revisited approaches, Biotechnol. Adv. 33 (2015) 1342-1354.

[2] N. Islam, V. Ferro. Recent advances in chitosan-based nanoparticulate pulmonary drug delivery. Nanoscale, 30 (2016), 14341-14358.

[3] R. Iyer, C. CW Hsia, K. T Nguyen. (2015). Nano-therapeutics for the lung: state-of-the-art and future perspectives. Curr Pharm Des, 36 (2015), 5233-5244.

[4] S.K. Shukla, A.K. Mishra, O.A. Arotiba, B.B. Mamba, Chitosan-based nanomaterials: a state-of-the-art review, Int J Biol Macromol. 59 (2013) 46–58.

[5] P. Agrawal, G.J. Strijkers, K. Nicolay, Chitosan-based systems for molecular imaging, Adv. Drug Deliv. Rev. 62 (2010) 42–58.

[6] Y. Pan, Y.J. Li, H.Y. Zhao, J.M. Zheng, H. Xu, G. Wei, J.S. Hao, F.D. Cui, Bioadhesive polysaccharide in protein delivery system: chitosan nanoparticles improve the intestinal absorption of insulin in vivo, Int J Pharm. 249 (2002) 139–147.

[7] L. Bugnicourt, P. Alcouffe, C. Ladavière, Elaboration of chitosan nanoparticles: Favorable impact of a mild thermal treatment to obtain finely divided, spherical, and colloidally stable objects, Colloids Surfaces A Physicochem. Eng. Asp. 457 (2014) 476–486.

[8] S. Mao, U. Bakowsky, A. Jintapattanakit, T. Kissel, Self□assembled polyelectrolyte nanocomplexes between chitosan derivatives and insulin, J. Pharm. Sci. 96 (2006) 1035-1048

[9] M.S. Alai, W.J. Lin, S.S. Pingale, Application of polymeric nanoparticles and micelles in insulin oral delivery, J. Food Drug Anal. 23 (2015) 351–358.

[10] K. Giger, R.P. Vanam, E. Seyrek, P.L. Dubin, Suppression of insulin aggregation by heparin, Biomacromolecules. 9 (2008) 2338–2344.

[11] G. Sharma, A.R. Sharma, J.-S. Nam, G.P.C. Doss, S.-S. Lee, C. Chakraborty, Nanoparticle based insulin delivery system: the next generation efficient therapy for Type 1 diabetes., J. Nanobiotechnology. 13 (2015) 74-87.

[12] M.K. Marschütz, A. Bernkop-Schnürch, Oral peptide drug delivery: Polymer-inhibitor conjugates protecting insulin from enzymatic degradation in vitro, Biomaterials. 21 (2000) 1499–1507.

[13] P. Mukhopadhyay, S. Chakraborty, S. Bhattacharya, R. Mishra, P.P. Kundu, PH-sensitive chitosan/alginate core-shell nanoparticles for efficient and safe oral insulin delivery, Int. J. Biol. Macromol. 72 (2015) 640–648.

[14] P. Mukhopadhyay, K. Sarkar, M. Chakraborty, S. Bhattacharya, R. Mishra, P.P. Kundu, Oral insulin delivery by self-assembled chitosan nanoparticles: In vitro and in vivo studies in diabetic animal model, Mater. Sci. Eng. C. 33 (2013) 376–382.

[15] L.G. Parada, R. Miranda, S. Salvador, Caracterización de quitosano por viscosimetría capilar y valoración potenciométrica, Rev. Iberoam. Polímeros. 5 (2004) 1–16.

[16] J. Li, Y. Wu, L. Zhao, Antibacterial activity and mechanism of chitosan with ultra high molecular weight, Carbohydr. Polym. 148 (2016) 200–205.

[17] D.W. Tang, S.H. Yu, Y.C. Ho, B.Q. Huang, G.J. Tsai, H.Y. Hsieh, H.W. Sung, F.L. Mi, Characterization of tea catechins-loaded nanoparticles prepared from chitosan and an

edible polypeptide, Food Hydrocoll. 30 (2013) 33–41.

[18] M. Weijers, F. Van De Velde, A. Stijnman, A. Van De Pijpekamp, R.W. Visschers, Structure and rheological properties of acid-induced egg white protein gels, Food Hydrocoll. 20 (2006) 146–159.

[19] I.A. Sogias, A.C. Williams, V. V. Khutoryanskiy, Why is chitosan mucoadhesive?, Biomacromolecules. 9 (2008) 1837–1842.

[20] A. Stirpe, M. Pantusa, B. Rizzuti, L. Sportelli, R. Bartucci, R. Guzzi, Early stage aggregation of human serum albumin in the presence of metal ions, Int. J. Biol. Macromol. 49 (2011) 337–342.

[21] O.E. Pérez, T. David-Birman, E. Kesselman, S. Levi-Tal, U. Lesmes, Milk protein–vitamin interactions: Formation of beta-lactoglobulin/folic acid nano-complexes and their impact on in vitro gastro-duodenal proteolysis, Food Hydrocoll. 38 (2014) 40–47.

[22] J. Moore, E. Cerasoli, Particle Light Scattering Methods and Applications, Encycl. Spectrosc. Spectrom. (2017) 543–553.

[23] R. Hunter, Foundations of colloid science, Oxford University Press, 2001.

[24] M. Rao, Flow and Functional Models for Rheological Properties of Fluid Foods, in: Rheology of Fluid, Semisolid, and Solid Foods, Food Engineering Series. Springer, Boston, 2014, pp. 27-61.

[25] A. Kumar Prusty, S.K. Sahu, Development and Evaluation of Insulin Incorporated Nanoparticles for Oral Administration, ISRN Nanotechnol.(2013) 1–6.

[26] Y. Xu, Y. Yan, D. Seeman, L. Sun, P.L. Dubin, Multimerization and Aggregation of Native State Insulin: Effect of Zinc, Langmuir. (2011) 579–586.

[27] M.F. Dunn, Zinc – ligand interactions modulate assembly and stability of the insulin hexamer – a review, BioMetals. 2 (2005) 295–303.

[28] O.E. Philippova, E. V. Volkov, N.L. Sitnikova, A.R. Khokhlov, J. Desbrieres, M. Rinaudo, Two types of hydrophobic aggregates in aqueous solutions of chitosan and its hydrophobic derivative, Biomacromolecules. 2 (2001) 483–490.

[29] A. Tsuboi, T. Izumi, M. Hirata, J. Xia, Complexation of Proteins with a Strong Polyanion in an Aqueous Salt-free System, Langmuir. 7463 (1996) 6295–6303.

[30] E. Smirnova, I. Safenkova, V. Stein-margolina, V. Shubin, V. Polshakov, B. Gurvits, Biochimie pH-responsive modulation of insulin aggregation and structural transformation of the aggregates, Biochimie. 109 (2015) 49–59.

[31] R. Coppolino, S. Coppolino, V. Villari, Study of the Aggregation of Insulin Glargine by Light Scattering, J. Pharm. Sci. 95 (2006) 1029–1034.

[32] M. Fandrich, V. Forge, K. Buder, M. Kittler, C.M. Dobson, S. Diekmann, Myoglobin forms amyloid fibrils by association of unfolded polypeptide segments, Proc. Natl. Acad. Sci. U. S. A. 100 (2003) 15463–15468.

[33] N.K. Holm, S.K. Jespersen, L. V. Thomassen, T.Y. Wolff, P. Sehgal, L.A. Thomsen, G. Christiansen, C.B. Andersen, A.D. Knudsen, D.E. Otzen, Aggregation and fibrillation of bovine serum albumin, Biochim. Biophys. Acta - Proteins Proteomics. 1774 (2007) 1128–1138.

[34] D. Hamada, C.M. Dobson, A kinetic study of β-lactoglobulin amyloid fibril formation promoted by urea, J. Agric. Food Chem. 11 (2014) 595–606.

[35] O.E. Perez, A.M.R. Pilosof, Pulsed electric fields effects on the molecular structure and gelation of beta-lactoglobulin concentrate and egg white, Food Res. Int. 37 (2004) 102–110.

[36] X.T. Le, L. Rioux, S.L. Turgeon, Formation and functional properties of protein – polysaccharide electrostatic hydrogels in comparison to protein or polysaccharide hydrogels, Adv. Colloid Interface Sci. 239 (2017) 127–135.

[37] J. Juarez, S.G. Lopez, A. Cambon, P. Taboada, V. Mosquera, Influence of Electrostatic Interactions on the Fibrillation Process of Human Serum Albumin, J. Phys. Chem. B. 113 (2009) 10521–10529.

[38] M.I. Ltd, Protein Characterization Using Dynamic & Static Light Scattering Techniques From Malvern Instruments, (09.24.2016).

[39] C.D. Hoemann, D. Fong, Immunological responses to chitosan for biomedical 38] A. Matalanis, O.G. Jones, D.J. McClements, Structured biopolymer-based delivery systems for encapsulation, protection, and release of lipophilic compounds, Food Hydrocoll. 25 (2011) 1865–1880.

[40] W.D. Kohn, R. Micanovic, S.L. Myers, A.M. Vick, S.D. Kahl, L. Zhang, B.A. Strifler, S. Li, J. Shang, J.M. Beals, J.P. Mayer, R.D. DiMarchi, pI-shifted insulin analogs with extended in vivo time action and favorable receptor selectivity, Peptides. 28 (2007) 935–948.

[41] Q.T. Ho, J. Carmeliet, A.K. Datta, T. Defraeye, M.A. Delele, E. Herremans, L. Opara, H. Ramon, E. Tijskens, R. Van Der Sman, P. Van Liedekerke, P. Verboven, B.M. Nicolaï, Multiscale modeling in food engineering, J. Food Eng. 114 (2013) 279–291.

[42] S. Bhattacharjee, Review article DLS and zeta potential – What they are and what they are not ?, J. Control. Release. 235 (2016) 337–351.

[43] A. Portero, C. Remuñán-López, H.M. Nielsen. The potential of chitosan in enhancing peptide and protein absorption across the TR146 cell culture model—an in vitro model of the buccal epithelium. Pharm. Res., 2 (2002), 169-174.

[44] M. Karimi, P. Avci, R. Mobasseri, M.R. Hamblin, H. Naderi-Manesh, The novel albumin-chitosan core-shell nanoparticles for gene delivery: Preparation, optimization and cell uptake investigation, J. Nanoparticle Res. 15 (2013) 1651-1665.

[45] N. Reddy, R. Reddy, Q. Jiang, Crosslinking biopolymers for biomedical applications, Trends Biotechnol. 33 (2015) 362–369.

[46] L.P. Martínez-Padilla, J.L. García-Rivera, V. Romero-Arreola, N.B. Casas-Alencáster, Effects of xanthan gum rheology on the foaming properties of whey protein concentrate, J. Food Eng. 156 (2015) 22–30.

[47] B. M. McKenna and J. G. Lyng, Rheological measurements of foods, in: Instrum. Tech. Qual. Control Lab., University College Dublin, 2001.

[48] H. Bohidar, P.L. Dubin, P.R. Majhi, C. Tribet, W. Jaeger, Effects of protein− polyelectrolyte affinity and polyelectrolyte molecular weight on dynamic properties of bovine serum albumin− poly (diallyldimethylammonium chloride) coacervates. Biomacromolecules, 6 (2005), 1573-1585.

[49] M.I. Ltd, Size Measurement and Molecular Weight Estimation of Globins using Dynamic Light Scattering From Malvern Instruments, (03.17.2017).

[50] S.P. Poulos, M. V Dodson, G.J. Hausman, Cell line models for differentiation: preadipocytes and adipocytes, Experimental Biology and Medicine, 235 (2012) 1185–1193.

[51] J. Giudice, L.S. Barcos, F.F. Guaimas, A. Penas-Steinhardt, L. Giordano, E. a Jares-Erijman, F. Coluccio Leskow, Insulin and insulin like growth factor II endocytosis and signaling via insulin receptor B., Cell Commun. Signal. 11 (2013) 18.

[52] J. Giudice, E.A. Jares-Erijman, F.C. Leskow, Endocytosis and Intracellular Dissociation Rates of Human Insulin − Insulin Receptor Complexes by Quantum Dots in Living Cells, Bioconjugate Chem. 24 (2013) 431-442.

Figure captions

Fig. 1**.** Time dependence of the absorbance at 500 nm for CS solutions registered (a) pH 2 and 6 (b) and I-CS mixed solutions at pH 2 and (c) pH 6. Pure protein solution concentration, 0.2 %, w/w, was monitored for comparison. CS concentrations in mixed solutions were $1 \cdot 10^{-4}$, $1 \cdot 10^{-3}$ and $1 \cdot 10^{-2}$%, w/w. Temperature: 25 °C.

Fig. 2. Volume particle size distribution (based on DLS data) of (a) Insulin at pH 2 and pH 6. (b) Curves obtained for I-CS nano-complexes at pH2 (c) and pH 6. Pure protein solution, 0.2 %, w/w, was monitored for comparison. CS concentrations in mixed solutions were $1 \cdot 10^{-4}$, $1 \cdot 10^{-3}$ and $1 \cdot 10^{-2}$ %, w/w. Temperature for DLS measurements was 25 °C.

Fig. 3. Influence of pH on the electrical charge (ζ-potential) of solutions containing Insulin and Chitosan $1 \cdot 10^{-3}$%, w/w. Shaded zone in the graph indicates the highest probability for the electrostatic interactions between molecules. Temperature: 25 °C.

Fig. 4. ζ -potential values of Insulin, 0.2%, w/w, with variable concentration of chitosan (I-CS), compared with samples containing pure chitosan, at pH 6. Measurements were performed after 3 hours of I-CS mixtures preparation. Black arrow indicates pure Insulin ζ-potential. Temperature: 25 °C.

Fig. 5. Flow curves for (a) I-CS mixed solutions and (b) viscosity, registered at pH 6. Pure protein solution concentration, 0.2 %, w/w, was included for comparison. CS concentrations in mixed solutions were $1 \cdot 10^{-4}$, $1 \cdot 10^{-3}$ and $1 \cdot 10^{-2}$%, w/w. Temperature of measurements 25 °C.

Fig. 6. Scheme showing the configuration events occurring during I-CS nano-complexation as modulated by the pH of mixed solution and CS concentration. (a) CS concentration 1·10-2% with no association between I dimers and CS, at pH<pI of I. Core-shell nanostructures at pH>pI. (b) CS concentration<1·10-

2%. No association between I dimers and CS, at pH<pI I-CS systems. Nano-complexes of different structures were formed by macromolecular entanglements at pH>pI.

Fig. 7. (a) Western blot showing changes in phosphorylated AKT levels after I or core-shell I-CS (1·10-2% CS) stimulation assayed in 3T3-L1 fibroblasts upon time. (b) Quantification of AKT activation over time showing a sustained increase for I-CS activation after two hours of stimulation.